Expert Systems with Applications 39 (2012) 10681–10692

Contents lists available at SciVerse ScienceDirect

Expert Systems with Applications

journal homepage: www.elsevier.com/locate/eswa

Fatigue crack growth estimation by relevance vector machine

Enrico Zio [a,b], Francesco Di Maio [b,*]

[a] Ecole Centrale Paris and Supelec, Grande Voie des Vignes, 92295 Chatenay-Malabry Cedex, France
[b] Energy Department, Politecnico di Milano, Via Ponzio 34/3, 20133 Milano, Italy

ARTICLE INFO

Keywords:
Prognostics
Residual useful life
Bayesian techniques
Relevance vector machine
Support vector machine
Fatigue crack growth

ABSTRACT

The investigation of damage propagation mechanisms on a selected safety–critical component or structure requires the quantification of its remaining useful life (RUL) to verify until when it can continue performing the required function. In this work, a relevance vector machine (RVM), that is a Bayesian elaboration of support vector machine (SVM), automatically selects a low number of significant basis functions, called relevant vectors (RVs), for degradation model identification, degradation state regression and RUL estimation. In particular, RVM capabilities are exploited to provide estimates of the RUL of a component undergoing crack growth, within an original combination of data-driven and model-based approaches to prognostics. The application to a case study shows that the proposed approach compares well to other methods (the model-based Bayesian approach of particle filtering and the data-driven fuzzy similarity-based approach) with respect to computational demand, data requirements, accuracy and that its Bayesian setting allows representing and propagating the uncertainty in the estimates.

1. Introduction

1.1. Motivation

Equipment degradation and unexpected failures impact the three key elements of production competitiveness, i.e., safety, cost and quality. In safety–critical applications, e.g., those of the aerospace, process and nuclear industries, it is even more important to rely upon well-maintained components in order to reduce downtime for the sake of plant safety and overall performance efficiency. Since often machines go through degradation before failure, monitoring and predicting the trend of their degradation and condition may allow correction before failure.

Indeed, when the conditions of a component or structure can be monitored, maintenance can be planned dynamically (Marseguerra, Zio, & Podofillini, 2002; Williams, Davies, & Drake, 1994). By predicting the future evolution of the degradation state of the component or structure, it is possible to verify whether it can continue performing the required function and, in case it cannot, estimate the remaining useful life (RUL), i.e., the time remaining before it can no longer perform its function (Jardine, Lin, & Banjevic, 2006). In practice, the estimate of the RUL may be difficult to obtain because the degradation state may not be directly observable and/or the measurements may be affected by noise and disturbances.

Approaches to prognostics for failure prediction can be categorized broadly into model-based and data-driven (Chiang, Russel, & Braatz, 2001).

1.2. Model-based approaches

Model-based prognostics attempts to set up physical models of the component or structure for the estimation of the RUL. Uncertainty due to the assumptions and simplifications of the adopted models may pose limitations to this approach. Many researchers have focused on the problem of building exhaustive models of deteriorating components and structures to implement model-based prognostic tools. Markov and semi-Markov models have been widely exploited for achieving analytical results (Baruah & Chinnam, 2005; Bérenguer, Grall, & Castanier, 2000; Dong & He, 2007; Grall, Bérenguer, & Chu, 1998; Hontelez, Burger, & Wijnmalen, 1996; Kopnov, 1999; Lam & Yeh, 1994; Samanta, Vesely, Hsu, & Subudly, 1991; Yeh, 1997). On the basis of these models, several approaches have been proposed to analyze reliability-based and condition-based maintenance policies (Castanier, Bérenguer, & Grall, 2002; Chen & Trivedi, 2005; Pulkkinen & Uryas'ev, 1992; Vlok, Coetzee, Banjevic, Jardine, & Makis, 2002).

The most promising approaches rely on Bayesian methods to combine a prior distribution of the unknown degradation states with the likelihood of the observations collected, to build a posterior distribution (Caesarendra, Niu, & Yang, 2010; Doucet, 1998; Doucet, de Freitas, & Gordon, 2001). In this setting, the estimation method most frequently used in practice is the Kalman filter, which is optimal for linear state space models and independent,

* Corresponding author.
E-mail addresses: enrico.zio@ecp.fr, enrico.zio@supelec.fr (E. Zio), enrico.zio@polimi.it, f.dimaio@mail.polimi.it (F. Di Maio).

0957-4174/$ - see front matter © 2012 Elsevier Ltd. All rights reserved.
http://dx.doi.org/10.1016/j.eswa.2012.02.199

additive Gaussian noises (Anderson & Moore, 1979). In this case, the posterior distributions are also Gaussian and computed exactly, without approximations. However, in most realistic cases the dynamics of degradation is non linear and/or the associated noises are non-Gaussian. Various approximate methods can be proposed to tackle these cases, e.g., the analytical approximations of the extended Kalman (EKF) and the Gaussian-sum filters and the numerical approximations of the grid-based filters (Anderson & Moore, 1979). Recently, Monte Carlo sampling methods are gaining popularity for their flexibility and ease of design (Kitagawa, 1987). These methods go under the name of particle filtering because the continuous distributions of interest are approximated by a discrete set of weighed particles, where each particle represents a random trajectory of evolution in the state space and the weight is the probability of the trajectory (Cadini, Zio, & Avram, 2009; Djuric et al., 2003; Doucet, Godsill, & Andreu, 2000).

1.3. Data-driven approaches

Data-driven techniques utilize monitored operational data related to system health. They can be beneficial when understanding of first principles of system operation is not straightforward or when the system is so complex that developing an accurate model is prohibitively expensive.

Data-driven techniques can be divided into two categories: statistical techniques (regression methods, ARMA models, etc.) and artificial intelligence (AI) techniques (neural networks (NNs), fuzzy systems (FSs), etc.). The most direct data-driven techniques for RUL estimation attempts at fitting available data of component or structure degradation by regression models and then extrapolating the evolution up to failure. However, in practice, the component or structure degradation history available may be short and incomplete, and extrapolation may lead to large errors (Yan, Koç, & Lee, 2004).

With respect to AI techniques, the most commonly used prediction methods are based on NNs (Barlett & Uhrig, 1992; Peel, 2008; Santosh, Srivastava, Sanyasi Rao, Gosh, & Kushwaha, 2009). For prognostic tasks, promising methods are recurrent NNs (Campolucci, Uncini, Piazza, & Rao, 1999; More & Deo, 2003), Neuro-Fuzzy systems (Tran, Yang, & Tan, 2009; Wang, Goldnaraghi, & Ismail, 2004) and support vector machines (SVMs) Sotiris & Pecht, 2007. In spite of the recognized potential of empirical, data-driven techniques, limitations still exist for their use in safety–critical applications, e.g., in nuclear technology, because of the lack of a systematic approach for selecting the structure and parameters of the models and their black-box character which limits intuition with respect to the understanding of their performance (Wang, Yu, Siegel, & Lee, 2008).

1.4. A combined model-based and data-driven approach

In the attempt to benefit from specific advantages of data-driven and model-based approaches, in this paper we propose a novel approach which combines relevance vector machine (RVM) and model fitting.

RVM is a Bayesian framework, of same functional form as SVM (Drucker, Burges, Kaufman, Smola, & Vapnik, 1997), for obtaining sparse solutions to regression and classification tasks utilizing models linear in the parameters (Fletcher, 2008; Tipping, 2001). The key feature is that it offers good generalization performance through sparse predictors, which contain relatively few non-zero basis functions, the so called relevant vectors (RVs). The majority of parameters are automatically set to zero during the learning process, giving a procedure that is extremely effective at discerning those basis functions which are relevant for making good predictions and avoiding over-fitting (Tipping, 2001). Then, a model is fitted to the selected RVs, to anticipate operational conditions and predict the future states of the process under study. In the case of interest in this work, this modeling scheme is used to provide estimates of the RUL of a component or structure undergoing degradation.

The combined approach has the potential to improve conventional methods, which are either purely data-driven methods not incorporating any physics of the process into the computation or solely model-based approaches which cannot accommodate for un-modeled effects and can diverge quickly in the presence of unanticipated operating conditions. Furthermore, the Bayesian approach underpinning RVM is well suited to handle uncertainty since it stands on probability distributions over both parameters and variables, and integrates out the nuisance terms (Caesarendra, Widodo, & Yang, 2010; Fletcher, 2008; Tipping, 2001).

The applicative focus of the present paper is the estimation of the RUL of an equipment subject to a non-linear fatigue crack growth process, typical for a certain class of industrial and structural components (Bolotin, Babkin, & Belousov, 1998; Myotyri, Pulkkinen, & Simola, 2006; Oswald & Schueller, 1984; Sobezyk & Spencer, 1992), on the basis of measurements of its degradation state taken at predefined inspection times (which are likely to be only few in practice due to the fact that the lower the number of measurements, the lower the computational time and the cost associated to the inspection procedures).

The paper contents are structured as follows. Section 2 contains the description of the approach at the basis of the RUL estimation, with an overview of the RVM framework. Section 3 presents the dynamic model of fatigue crack growth. In Section 4, the results of the application of the approach to a case study are presented, and an evaluation of the performance evaluation of the prognostic algorithm is given. Finally, some conclusions on the advantages and limitations of the approach here propounded are given in Section 5.

2. Methodology

Starting from time $t = 1$ throughout the time horizon of observation T, it is assumed that J successive measurements f_j, $j = 1,2,\ldots,J$ are taken at predefined inspection times T_j along a degradation-to-failure trajectory developing in the component or structure under analysis. At each T_j, the RUL estimation for the degrading component or structure is performed by resorting to a combination of RVM followed by model fitting and parameter estimation onto the identified RVs. Figs. 1 and 2 show a schematic sketch and a pseudocode of the novel computational framework, with reference to degradation signal $f(t)$, respectively.

2.1. Data collection

The first step consists in extracting the feature $f(t)$ from sensor data. For simplicity of illustration, we consider a single feature as the degradation signal used for estimating the component evolution towards failure.

2.2. Degradation model development

The degradation signal $f(t)$ is monitored throughout the time horizon of observation T, starting from (discrete) time $t = 1$; inspections of the component or structure degradation state, as indicated by signal $f(t)$, are made at predefined inspection times $(T_1, T_2, T_3, \ldots, T_J)$, where, computationally, $T_j - T_{j-1} = n$ is the number of discrete time steps between two successive inspections.

At each inspection time T_j, $j = 1,2,\ldots,J$, the last value $f(T_j)$ is recorded and appended to the vector of the values collected at the

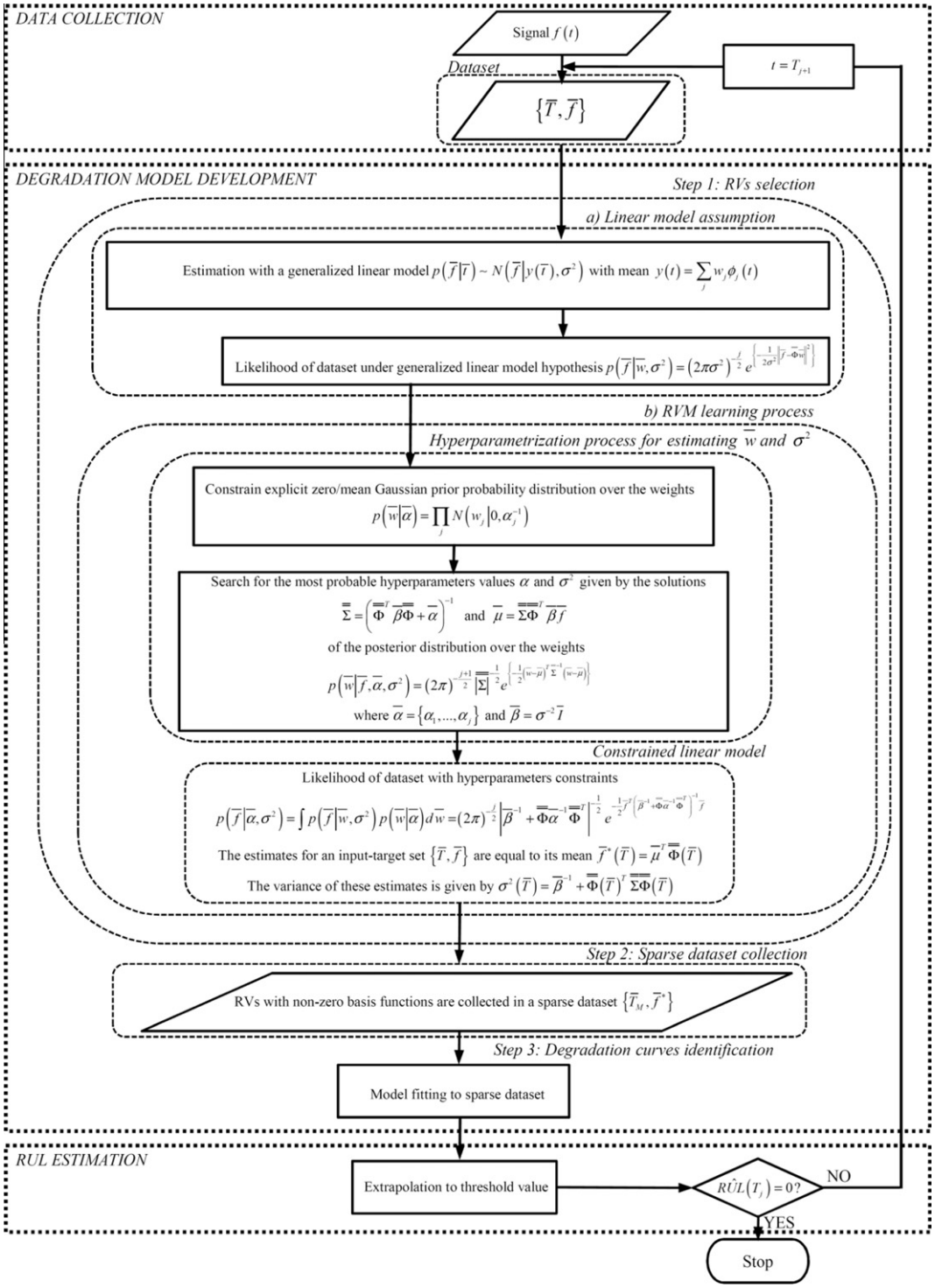

Fig. 1. Flowchart of the RUL estimation procedure.

previous $(j-1)$ inspections. Also, at each T_j, RVM regression is performed on the j available pairs of data $\{T_k,f_k\}$, where $k=1,2,\ldots,j$ and $f_k=f(T_k)$, so as to find the $M\leqslant j$ most representative pairs $\{T_l,f_l^*\}$, where, upon re-numbering, $l=1,2,\ldots,M$, and f_l^* is the state estimate provided by the RVM in correspondence of T_l. Then, fitting to the sparse dataset $\{T_l,f_l^*\}$ of non-zero basis functions is performed to identify the unknown parameters of the model adopted. Finally, the fitted model is extrapolated up to a pre-established failure threshold value d to evaluate the estimate $\hat{RUL}(T_j)$ of the RUL at time T_j, and its uncertainty.

Step 1: *Relevant vectors (RVs) selection*

(a) *Linear model assumption*

Given a set $\{T_k,f_k\}$ of j typically noisy measurements f_k at some points T_k, $k=1,2,\ldots,j$, a linear model can be used in a variety of regression cases:

```
SET failure threshold value
SET initial RVM hyperparameters values
SET estimated RUL equal to component Mean Time To Failure
SET inspection time equal to 1
WHILE estimated RUL is greater than 0
    INCREASE inspection time value
    TRAIN a sparse RVM model
    SELECT a set of important relevance vectors y_used corresponding to the inspection times t_used
    EVALUATE the RVM estimates at inspection times t_used
        SET y_rvm equal to the linear combination of the selected radial basis y_used
        SET standarddev of y_rvm equal to the square root of the diagonal of the covariance matrix provided by
            the RVM framework
    IF size y_used is smaller than 2 THEN
        SET the estimated RUL equal to trajectory total length minus inspection time
    ELSE
        FIT the Paris Erdogan model to the estimated degradation state y_rvm
        EVALUATE the Inverse Paris Erdogan model coefficients
        EVALUATE the time t_exceedance at which the curve exceeds the failure threshold
        SET the estimated RUL equal to t_exceedance minus inspection time
    ENDIF
ENDFOR
```

Fig. 2. Pseudocode of the RUL estimation procedure.

$$f(T_j) = y(T_j) + \varepsilon_j \tag{1}$$

where ε_j is the noise component of the measurement and the unknown function $y(t)$ is a linear combination of some known basis functions $\phi_j(t)$, i.e.,

$$y(t) = \sum_j w_j \phi_j(t) \tag{2}$$

The vector $\bar{w} = \{w_1, \ldots, w_j\}$ contains the linear combination weights. In many applications, the solution of Eq. (2) suffers of over-fitting. To overcome this, constraints can be introduced on the parameters $\bar{w} = \{w_1, \ldots, w_j\}$ to introduce desired properties of the estimated function. For example, in the RVM framework, smaller weight values leading to desirable smooth estimates and to a lower number $M \leqslant j$ of basis functions are preferable. This property is called sparseness and is useful for several reasons: *i*) sparse models can generalize well and are fast to compute and *ii*) they also provide a feature selection mechanism which can be useful in various applications. The M pairs of data $\{T_l, f_l^*\}, l = 1, 2, \ldots, M$, whose basis functions $\phi(T_l)$ have non-zero weights are called RVs (for further details, the interested reader can refer to Fletcher (2008).

(b) *RVM learning process*

(a) *Hyperparametrization for estimating $\bar{w}$ and σ^2*

The algorithm for identifying the RVs is based on hyperparametrization of the vector of weights $\bar{w}$. Indicating by $\overline{T} = \{T_1, T_2, \ldots, T_j\}$ and $\bar{f} = \{f_1, f_2, \ldots, f_j\}$ the vectors of inspection times and degradation states, respectively, we follow the standard formulation and assume that the conditional probability of the observations $\bar{f}$ at the inspection times $\overline{T}, p(\bar{f}|\overline{T})$ is Gaussian $N(\bar{f}|y(\overline{T}), \sigma^2)$, given Eq. (1) and assuming a constant noise variance σ^2. The likelihood of the dataset $\{\overline{T}, \bar{f}\}$ can then be written as:

$$p(\bar{f}|\bar{w}, \sigma^2) = (2\pi\sigma^2)^{-\frac{j}{2}} e^{\left\{-\frac{1}{2\sigma^2}\|\bar{f} - \overline{\overline{\Phi}}\bar{w}\|^2\right\}} \tag{3}$$

where $\overline{\overline{\Phi}}$ is the $j \times j$ 'design basis function' matrix.

Typically, higher-level parameters are introduced to constrain an explicit zero-mean Gaussian prior probability distribution over the weights (Tipping, 2001):

$$p(\bar{w}|\bar{\alpha}) = \prod_j N\left(w_j|0, \alpha_j^{-1}\right) \tag{4}$$

where $\bar{\alpha} = \{\alpha_1, \alpha_2, \ldots, \alpha_j\}$ is a vector of j hyperparameters that controls how far from zero each weight is allowed to deviate. Using Bayes' rule, the posterior overall unknowns can be computed, given the defined non-informative prior-distributions:

$$p(\bar{w}, \bar{\alpha}, \sigma^2|\bar{f}) = \frac{p(\bar{f}|\bar{w}, \bar{\alpha}, \sigma^2)p(\bar{w}, \bar{\alpha}, \sigma^2)}{\int p(\bar{f}|\bar{w}, \bar{\alpha}, \sigma^2)p(\bar{w}, \bar{\alpha}, \sigma^2)d\bar{w}d\bar{\alpha}d\sigma^2} \tag{5}$$

However, the solution of the posterior in Eq. (5) cannot be directly computed since one cannot perform the normalizing integral at the denominator. Instead, the posterior is decomposed as:

$$p(\bar{w}, \bar{\alpha}, \sigma^2|\bar{f}) = p(\bar{w}|\bar{f}, \bar{\alpha}, \sigma^2)p(\bar{\alpha}, \sigma^2|\bar{f}) \tag{6}$$

The posterior distribution of weights is given by

$$p(\bar{w}|\bar{f}, \bar{\alpha}, \sigma^2) = \frac{p(\bar{f}|\bar{w}, \sigma^2)p(\bar{w}, \bar{\alpha})}{p(\bar{f}|\bar{\alpha}, \sigma^2)} \tag{7}$$

Resorting to Bayes' rule, Eq. (7) can be written as:

$$p(\bar{w}|\bar{f}, \bar{\alpha}, \sigma^2) = (2\pi)^{-\frac{j+1}{2}}|\overline{\overline{\Sigma}}|^{-\frac{1}{2}} e^{\left\{-\frac{1}{2}(\bar{w}-\bar{\mu})^T\overline{\overline{\Sigma}}^{-1}(\bar{w}-\bar{\mu})\right\}} \tag{8}$$

whose covariance and mean are equal to, respectively:

$$\overline{\overline{\Sigma}} = \left(\overline{\overline{\Phi}}^T\bar{\beta}\overline{\overline{\Phi}} + \bar{\alpha}\right)^{-1} \tag{9}$$

$$\bar{\mu} = \overline{\overline{\Sigma\Phi}}^T\bar{\beta}\bar{f} \tag{10}$$

with the upper index T indicating the usual transpose operator and $\bar{\beta} = \sigma^{-2}\bar{I}$. Upon establishing a suitable convergence criteria for $\bar{\alpha}$ and $\bar{\beta}$, the problem becomes one of iterative searching for the most probable posterior hyper-parameters (Fletcher, 2008). The quantification of the optimal $\bar{\alpha}$, allows the identification of M values T_l, $l = 1, 2, \ldots, M$ (upon re-numbering), with non-zero weighted radial basis functions; actually, only these M inputs contribute to the state prediction in what follows and its vector is denoted by $\overline{T}_M$.

(b) *Constrained linear model*

State estimations can be made in terms of the predictor distribution

$$\begin{aligned} p(\bar{f}|\bar{\alpha}, \sigma^2) &= \int p(\bar{f}|\bar{w}, \sigma^2)p(\bar{w}|\bar{\alpha})d\bar{w} \\ &= (2\pi)^{-\frac{j}{2}}\left|\bar{\beta}^{-1} + \overline{\overline{\Phi}}\bar{\alpha}^{-1}\overline{\overline{\Phi}}^T\right|^{-\frac{1}{2}} e^{-\frac{1}{2}\bar{f}^T\left(\bar{\beta}^{-1}+\overline{\overline{\Phi}}\bar{\alpha}^{-1}\overline{\overline{\Phi}}^T\right)^{-1}\bar{f}} \end{aligned} \tag{11}$$

Given the dataset $\{\overline{T},\bar{f}\}$, the estimates $\bar{f}^*(\overline{T})$ are equal to the mean of Eq. (11):

$$\bar{f}^*(\overline{T}) = \bar{\mu}^T\overline{\overline{\Phi}}(\overline{T}) \tag{12}$$

whereas the variance relating to these estimates is given by

$$\sigma^2(\overline{T}) = \bar{\beta}^{-1} + \overline{\overline{\Phi}}(\overline{T})^T\overline{\overline{\Sigma\Phi}}(\overline{T}) \tag{13}$$

Because $p(\bar{f}|\overline{T})$ is Gaussian, the 99th and 1st percentiles of the prediction distribution $p(\bar{f}|\alpha,\sigma^2)$, i.e., $\bar{f}^*_{99}(\overline{T})$ and $\bar{f}^*_1(\overline{T})$, respectively, turn out to be equal to:

$$\bar{f}^*_{99/1}(\overline{T}) = \bar{f}^*(\overline{T}) \pm 3\sigma(\overline{T}) \tag{14}$$

Step 2: *Sparse dataset collection*
The M most representative estimated pairs $\{\overline{T}_M,\bar{f}^*\}$ found by the RVM regression, i.e., those RVs with non-zero basis functions, are collected in a sparse dataset.

Step 3: *Degradation curves identification*
The sparse dataset $\{\overline{T}_M,\bar{f}^*\}$ is used to fit the model for predicting the component or structure degradation; high and low uncertainty bounds are also provided by fitting the M estimates $\bar{f}^*_{99}(\overline{T}_M)$ and $\bar{f}^*_1(\overline{T}_M)$, respectively.

2.3. RUL estimation

The fitted model is used to predict the degradation signal value at the future time steps. Deviations from the nominal signal value can be easily detected, so that no independent fault detection module is needed to activate the prognostic module.

The estimated RUL at time T_j, $\hat{RUL}(T_j)$, is then derived by projecting into the future the M state estimates $\bar{f}^*(\overline{T}_M)$ until T^d, the time at which the state hits the predetermined failure threshold d (Fig. 3).

In parallel, lower and upper RUL uncertainty bounds ($\hat{RUL}_l(T_j)$ and $\hat{RUL}_u(T_j)$, respectively) are estimated by calculating the times T^d_{99} and T^d_1 when the model prediction curves fitted on $\bar{f}^*_{99}(\overline{T}_M)$ and $\bar{f}^*_1(\overline{T}_M)$ exceed the threshold d, respectively.

Thus, at time T_j the RUL is taken equal to:

$$\hat{RUL}_{u/l}(T_j) = \left(T^d - T_j\right) \pm \left(T^d_{u/l} - T_j\right) \tag{15}$$

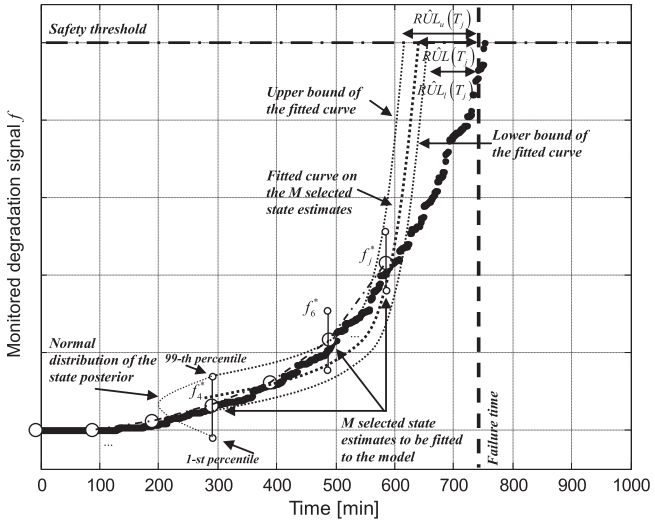

Fig. 3. The estimated remaining time before failure $\hat{RUL}(T_j)$ at time T_j, and its upper and lower uncertainty bounds $\hat{RUL}_u(T_j)$ and $\hat{RUL}_l(T_j)$, respectively. The degradation signal is assumed to be known by inspection at the times T_j; the white circles represent the state estimates $\bar{f}^*(\overline{T})$ at each inspection time T_j.

3. Application to a fatigue crack growth process

Let us consider a process of crack growth in a component subject to fatigue. The common Paris–Erdogan model is adopted for describing the evolution of the crack depth x as a function of the load cycles t (Pulkkinen, 1991):

$$\frac{dx}{dt} = C(\Delta S)^m \tag{16}$$

where C and m are constants related to the material properties (Kozin & Bogdanoff, 1989; Provan, 1987), which can be estimated from experimental data (Bigerelle & Iost, 1999) and ΔS is the stress intensity amplitude, roughly proportional to the square root of x Provan (1987), i.e., $\Delta S = \gamma\sqrt{x}$, where γ is again a constant which may be determined from experimental data.

Taking the logarithm of both sides of Eq. (16) and adding a white Gaussian noise $\omega \sim N(0,\sigma^2_\omega)$, the randomized Paris–Erdogan model is equal to (Myotyri et al., 2006):

$$\ln\frac{dx}{dt} = \ln C + m\ln(\Delta S) + \varepsilon \tag{17}$$

From Eq. (17), the intrinsic stochasticity of the process may be inserted in the model by modifying Eq. (16) as follows (Provan, 1987):

$$\frac{dx}{dt} = e^{\omega}C(\gamma\sqrt{x})^m \tag{18}$$

Note that Eq. (18) can be randomized also in other ways that lead to stochastic differential equations (Bigerelle & Iost, 1999), written as $\frac{dx}{dt} = e^{\omega+\ln C}(\gamma\sqrt{x})^m$, if the stochasticity of the process is associated to parameter C instead of ω.

For Δt sufficiently small, the state-space model (18) can be discretized to give:

$$x(t_k) = x(t_{k-1}) + e^{\omega_j}C(\Delta S)^m\Delta t \tag{19}$$

which represents a non-linear Markov process with independent, non-stationary degradation increments of the degradation state x.

At the generic inspection time T_j, the degradation state $x(T_j)$ is generally not directly measurable. In the case of non-destructive ultrasonic inspections a logit model for the observation $f(T_j)$ can be introduced (Simola & Pulkkinen, 1998):

$$\ln\frac{f(T_j)}{d-f(T_j)} = \gamma_0 + \gamma_1\ln\frac{x(T_j)}{d-x(T_j)} + \upsilon_k \tag{20}$$

where d is the component material thickness, $\gamma_0 \in (-\infty,\infty)$ and $\gamma_1 > 0$ are parameters to be estimated from experimental data and υ is a white Gaussian noise such that $\upsilon \sim N(0,\sigma^2_\upsilon)$.

The following standard transformations are introduced:

$$y(T_j) = \ln\frac{f(T_j)}{d-f(T_j)} \tag{21}$$

$$\mu(T_j) = \gamma_0 + \gamma_1\ln\frac{x(T_j)}{d-x(T_j)} \tag{22}$$

In the case study here considered, taken from Myotyri et al. (2006), the parameters of the state Eq. (19) are $C = 0.005$, $m = 1.3$ and $\gamma = 1$, whereas those in the measurement Eq. (20) are $\gamma_0 = 0.06$, and $\gamma_1 = 1.25$. The process and measurement noise variances are $\sigma^2_\omega = 2.89$ and $\sigma^2_\upsilon = 0.22$, respectively. The component is assumed failed when the crack depth $x \geqslant d = 100$, in arbitrary units. As an example, Fig. 4 shows the degradation-to-failure trajectory that in the following will be used as test trajectory in the procedure for predicting the component RUL. The crack depth x reaches the full material thickness $d = 100$ at 802 (min).

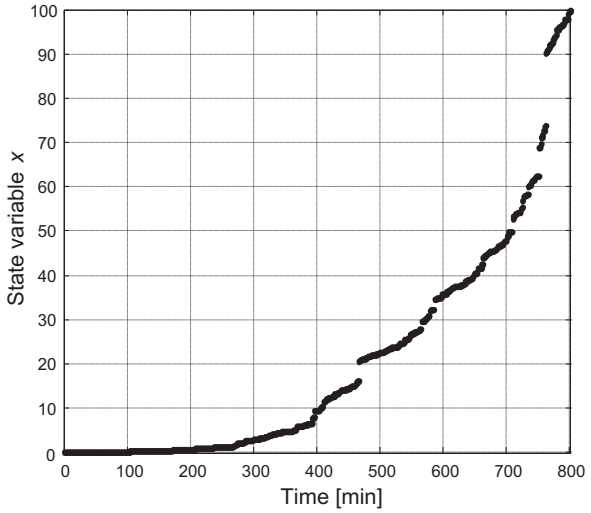

Fig. 4. Crack growth trajectory used as test trajectory.

4. Results

The application of the approach for computing at the inspection time T_j the estimate $\hat{RUL}(T_j)$ (Section 2) on the fatigue crack propagation case study (Section 3) is hereafter illustrated. The procedural steps are performed as follows:

4.1. Data collection

Starting from (discrete) time $t = 1$, the failure crack propagation signal $f(t)$ (Eq. (20)) is monitored throughout the time horizon of observation T; inspections of the degradation state of the component or structure are made at predefined inspection times ($T_1, T_2, T_3, \ldots, T_J$). The interval between two successive inspections is equal to $n = 50$ (min), to avoid too frequent and costly inspections of the component or structure integrity. At each inspection time T_j, $j = 1,2,\ldots,J$, the value $f(T_j)$ is recorded and appended to the vector of the values collected at the previous $(j-1)$th inspections.

4.2. Degradation model development

At each time T_j, RVM regression is performed on the pairs of data $\{T_k, f_k\}$, $k = 1,2,\ldots,j$, so as to find the M RVs $\{T_l, f_l^*\}, l = 1,2,\ldots,M$ (upon re-numbering). Then, the integral form of the Paris–Erdogan model is fitted to the sparse dataset $\{T_l, f_l^*\}$ by the identification of the unknown parameters m, C and γ of Eq. (18). Finally, the same fitted model is extrapolated to predict the time T_j at which the crack reaches its threshold value d, and the RUL estimate $\hat{RUL}(T_j)$; the lower and upper uncertainty bounds of the RUL estimate are also calculated, according to Eq. (15).

Step 1: *Relevant vectors (RV) selection*

(a) *Linear model assumption*
The unknown function $y(t)$ (Eq. (21)) is assumed to be a linear combination of some gaussian basis functions $\phi_j(t)$ weighted by w_j, according to Eq. (2), whose calculated values $\bar{w} = \{w_1, \ldots, w_j\}$ are reported in Table 1, at each inspection time.

(b) *RVM learning process*

(a) *Hyperparametrization for estimating $\bar{w}$ and σ^2*
The hyper parameters $\bar{\alpha} = \{\alpha_1, \ldots, \alpha_j\}$ and σ^2 are estimated during the machine learning process based on the data $\{T_k, f_k\}$, $k = 1,2,\ldots,j$, resorting to Eqs. (9) and (10).

Table 1
Weight values calculated during the machine learning process.

	T_1	T_2	T_3	T_4	T_5	T_6	T_7	T_8	T_9	T_{10}	T_{11}	T_{12}	T_{13}	T_{14}	T_{15}	T_{16}
$\bar{w} =$	$\begin{Bmatrix} w_1 \\ \vdots \\ w_j \end{Bmatrix}$	$\begin{Bmatrix} 0 \\ 0 \end{Bmatrix}$	$\begin{Bmatrix} 0 \\ 0 \\ 6 \end{Bmatrix} 10^{-2} \times$	$\begin{Bmatrix} 0 \\ 0 \\ 6 \\ 13 \end{Bmatrix} 10^{-2} \times$	$\begin{Bmatrix} -6 \\ -5 \\ 0 \\ 7 \\ 18 \end{Bmatrix} 10^{-2} \times$	$\begin{Bmatrix} -14 \\ -13 \\ -7 \\ 0 \\ 10 \\ 38 \end{Bmatrix} 10^{-2} \times$	$\begin{Bmatrix} -6 \\ -5 \\ 7 \\ 0 \\ 18 \\ 46 \\ 133 \end{Bmatrix} 10^{-2} \times$	$\begin{Bmatrix} -5 \\ -5 \\ 0 \\ 7 \\ 19 \\ 46 \\ 134 \\ 253 \end{Bmatrix} 10^{-2} \times$	$\begin{Bmatrix} 0 \\ 0 \\ 0 \\ 0 \\ 0 \\ 123 \\ 244 \\ 614 \end{Bmatrix} 10^{-1} \times$	$\begin{Bmatrix} 0 \\ 0 \\ 0 \\ 0 \\ 2 \\ 4 \\ 13 \\ 25 \\ 62 \\ 106 \end{Bmatrix} 10^{-1} \times$	$\begin{Bmatrix} 0 \\ 0 \\ 0 \\ 0 \\ 2 \\ 4 \\ 13 \\ 25 \\ 62 \\ 116 \\ 198 \end{Bmatrix}$	$\begin{Bmatrix} 0 \\ 0 \\ 0 \\ 0 \\ 0 \\ 0 \\ 1 \\ 2 \\ 6 \\ 10.5 \\ 19.2 \\ 23.8 \end{Bmatrix}$	$\begin{Bmatrix} 0 \\ 0 \\ 0 \\ 0 \\ 0 \\ 0.42 \\ 1.31 \\ 2.51 \\ 6.21 \\ 10.5 \\ 19.3 \\ 23.8 \\ 34.8 \end{Bmatrix}$	$\begin{Bmatrix} 0 \\ 0 \\ 0 \\ 0 \\ 0 \\ 0 \\ 1.23 \\ 2.44 \\ 6.14 \\ 10.5 \\ 19.2 \\ 23.8 \\ 34.7 \\ 40.6 \end{Bmatrix}$	$\begin{Bmatrix} 0 \\ 0 \\ 0 \\ 0 \\ 0 \\ 0 \\ 1.23 \\ 2.44 \\ 6.14 \\ 10.5 \\ 19.2 \\ 23.8 \\ 34.7 \\ 40.6 \\ 49.9 \end{Bmatrix}$	$\begin{Bmatrix} 0 \\ 0 \\ 0 \\ 0 \\ 0 \\ 0.1 \\ 0.47 \\ 1.35 \\ 2.55 \\ 6.24 \\ 10.6 \\ 19.3 \\ 23.9 \\ 34.8 \\ 40.6 \\ 50.0 \end{Bmatrix}$	$\begin{Bmatrix} -19 \\ -19 \\ -19 \\ -19 \\ -19 \\ -18 \\ -18 \\ -16 \\ -13 \\ -8 \\ 0 \\ 4.5 \\ 15.4 \\ 21.3 \\ 30.6 \\ 48.4 \\ 80.4 \end{Bmatrix}$

(b) *Constrained linear model*
The mean value of the predicted state value and its variance are calculated by Eqs. (12) and (13).

Step 2: *Sparse dataset collection*
The M most representative RVs $\{T_l, f_l^*\}, l = 1, 2, \ldots, M$ are collected in a sparse dataset.

Step 3: *Ageing curve identification*
The sparse dataset is used for fitting the Paris–Erdogan model of crack growth propagation. High and low uncertainty bounds are also provided by fitting $\bar{f}^*_{99}(\overline{T}_M)$ and $\bar{f}^*_1(\overline{T}_M)$, respectively.

4.3. RUL estimation

Integrating Eq. (18), the time of threshold exceedance T^d is equal to

$$T^d = \left(\frac{2-m}{2} A f\right)^{\frac{2}{2-m}} \tag{23}$$

where $A = e^{\omega} C(\gamma)^m$. The values of A and m are given in Table 2, at each inspection time. At time T_j, the RUL estimate $\hat{RUL}(T_j)$ and its upper and lower uncertainty bounds $\hat{RUL}_{u/l}(T_j)$ are computed according to Eq. (15).

The linear RVM regression and the Paris–Erdogan growth model fitted to the RVs for the crack propagation trajectory plotted in Fig. 4 are shown in Figs. 5–20, in correspondence of the successive inspection times T_j until failure. The interval between two successive inspections is equal to $n = 50$ (min); the circles are the M RVs collected at each inspection time T_j; the thin continuous line represents the fitted model degradation curve; the thin dashed lines are the upper and lower uncertainty bounds; the bold-dotted horizontal line indicates the failure threshold d. Note that the use of probabilistic kernels in RVM varies the number of RVs at the different time steps.

In Fig. 21, the $\hat{RUL}(T_j)$ estimates (second column of Table 3) for the crack propagation trajectory of Fig. 4 are plotted in bold circles together with their uncertainty interval of 99% confidence (third column of Table 3), plotted in dotted lines; at the beginning of the test trajectory, at each inspection time T_j the predictions match the mean time to failure $MTTF(T_j) = T - T_j$, where T is the time horizon of observation; then, when the signal is detected to deviate from its nominal value at time T_{det}, the $\hat{RUL}(T_j)$ estimate moves away from the $MTTF(T_j)$ values towards the real RUL (fourth column of Table 3), plotted in dashed-thick line. In the figure, the bold vertical line indicates the time of crack depth exceedance of the failure threshold.

The computational time required for the estimation along one complete degradation trajectory of 1000 [m] is of few seconds on an Intel® Atom 1.6 GHz.

4.4. Prognostic performance evaluation

In practice, it is necessary to know how good the prognostic estimates are before establishing a maintenance schedule to control degradation and/or counteracting actions against failure. A critical issue is then the definition of a significant indicator of prognostic performance.

Several metrics have been proposed to quantify the performance of prognostic algorithms (Goebel & Bonissone, 2005; Hyndman & Koehler, 2006; Makridakis & Hibon, 2000; Vachtsevanos, Lewis, Roemer, Hess, & Wu, 2006). These metrics help assess how well prediction estimates improve over time as more measurement data become available. In this work, we evaluate performance based on the Prognostic Horizon (PH) metric (Saxena, Celaya, Saha, Saha, & Goebel, 2009). The basic idea is that longer PH allows for more time to act based on a prediction that has some credibility. Correspondingly, PH is defined as the difference between the current time index j and the instance i when the prediction crosses the failure threshold; this definition may be supplied with an allowable error bound δ around the true T^d.

PH ensures that the predicted estimates are within specified limits around the actual T^d and hence the predictions may be considered trustworthy. For instance, a PH with error bound of $\delta = 5\%$ identifies when a given algorithm starts predicting estimates that are within 5% of T^d.

In Fig. 22, both the ±5% and ±10% error bounds with respect to T^d are given. The prediction for the failure crack growth degradation trajectory of Fig. 4 enters the 90% and 80% accuracy zone at 50%

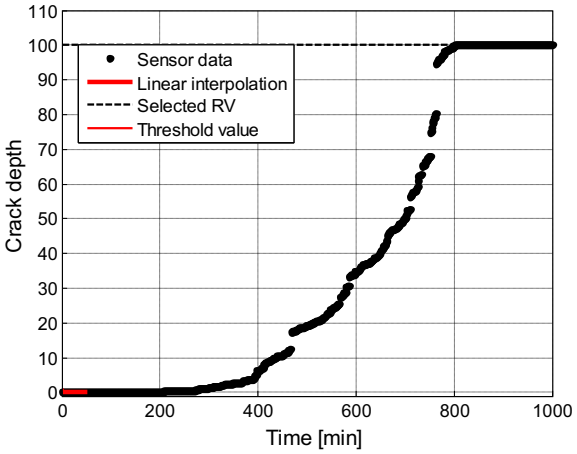

Fig. 5. Inspection time $T_1 = 50$ (min).

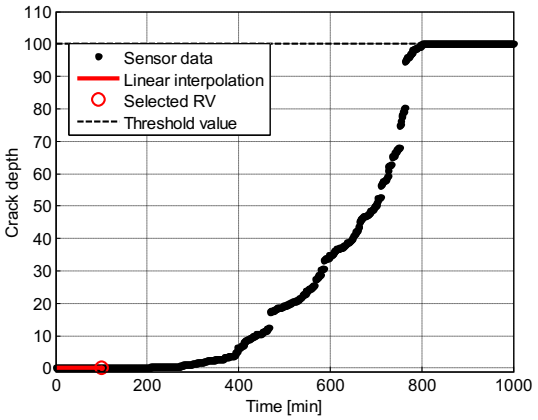

Fig. 6. Inspection time $T_2 = 100$ (min).

Table 2
Values of the parameters A and m of the integral Paris–Erdogan degradation model (Eq. (23)), at each inspection time.

	T_1	T_2	T_3	T_4	T_5	T_6	T_7	T_8	T_9	T_{10}	T_{11}	T_{12}	T_{13}	T_{14}	T_{15}	T_{16}
A	/	/	/	0.005	0.009	0.016	0.015	0.021	0.018	0.018	0.016	0.016	0.015	0.015	0.015	0.15
m	/	/	/	1.053	1.34	1.57	1.53	1.66	1.60	1.62	1.52	1.50	1.43	1.39	1.41	1.50

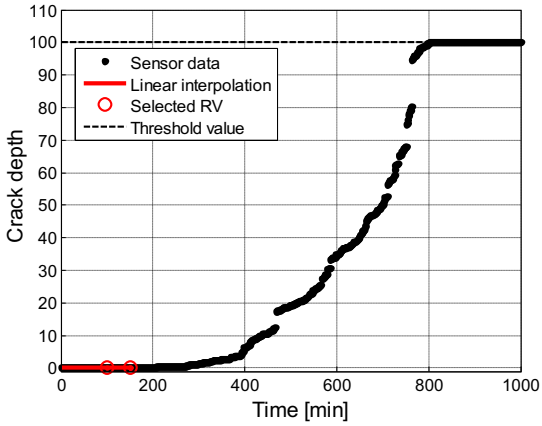

Fig. 7. Inspection time $T_3 = 150$ (min).

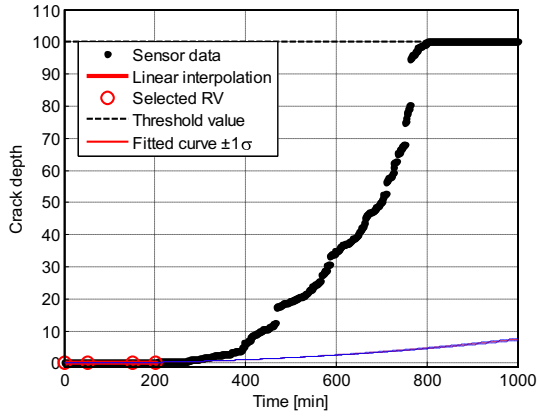

Fig. 8. Inspection time $T_4 = 200$ (min).

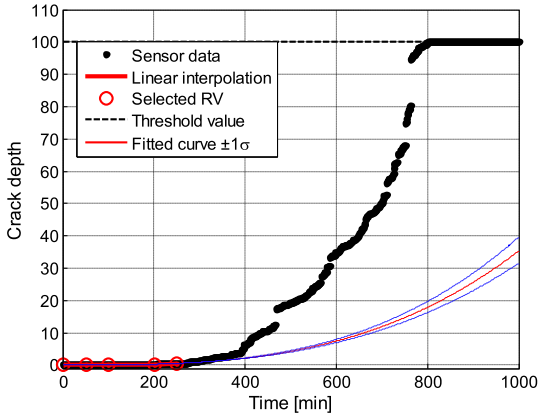

Fig. 9. Inspection time $T_5 = 250$ (min).

and 80% of the residual life after the degradation process has been detected, respectively. This indicates that the proposed method can give an high informative prediction at a sufficiently early stage of the component or structure life, so as to allow for preventive maintenance actions.

4.5. Comparison with other methods

The case study here illustrated has been analyzed with two other methods: the model-based Bayesian approach of particle filtering (PF) (Cadini et al., 2009) and the data-driven fuzzy similarity-based approach (FSBA) (Zio & Di Maio, 2010).

PF is a Monte Carlo simulation method designed to estimate and track, within a Bayesian framework, the state of a dynamic system, when the model parameters can be a priori estimated from data and then updated when additional measurements are collected. This model-based method is particularly suitable in those realistic cases where the dynamics of degradation is non-linear

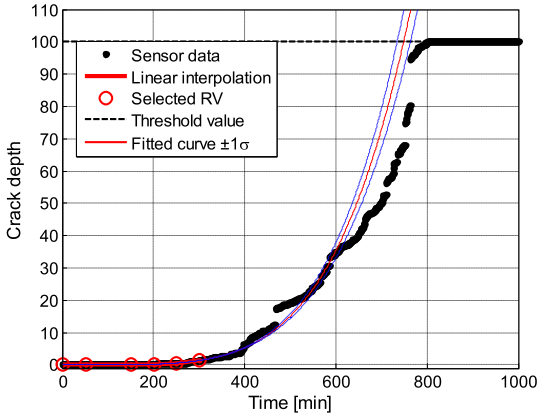

Fig. 10. Inspection time $T_6 = 300$ (min).

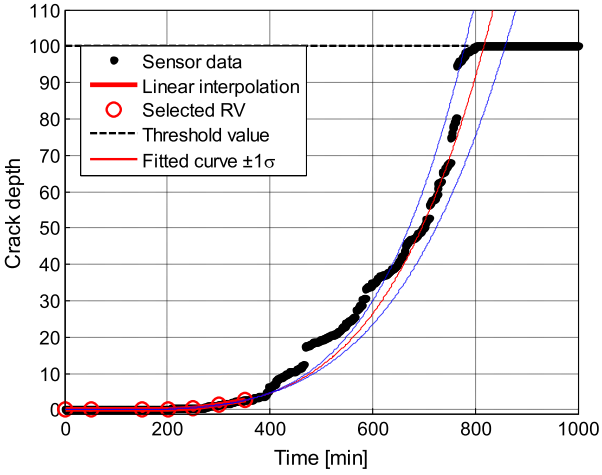

Fig. 11. Inspection time $T_7 = 350$ (min).

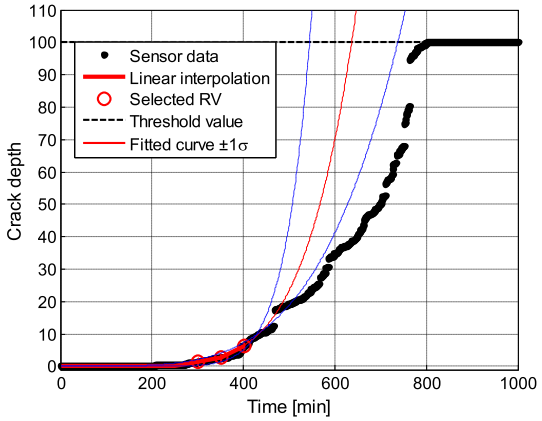

Fig. 12. Inspection time $T_8 = 400$ (min).

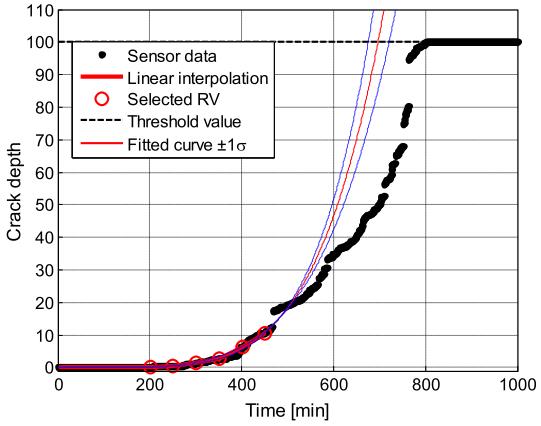

Fig. 13. Inspection time $T_9 = 450$ (min).

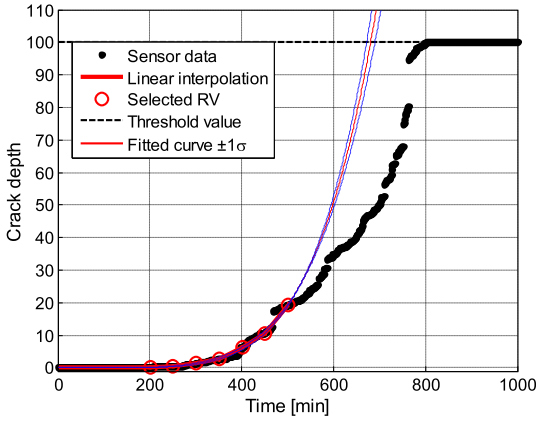

Fig. 14. Inspection time $T_{10} = 500$ (min).

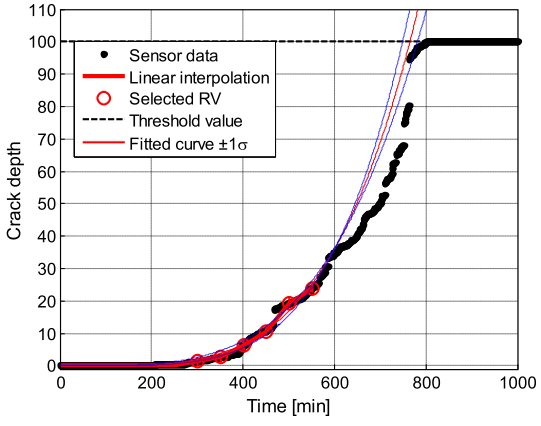

Fig. 15. Inspection time $T_{11} = 550$ (min).

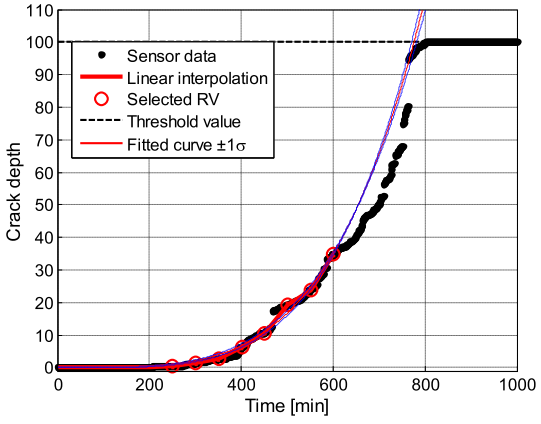

Fig. 16. Inspection time $T_{12} = 600$ (min).

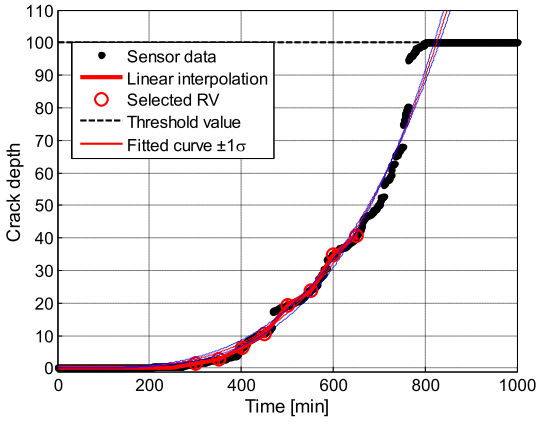

Fig. 17. Inspection time $T_{13} = 650$ (min).

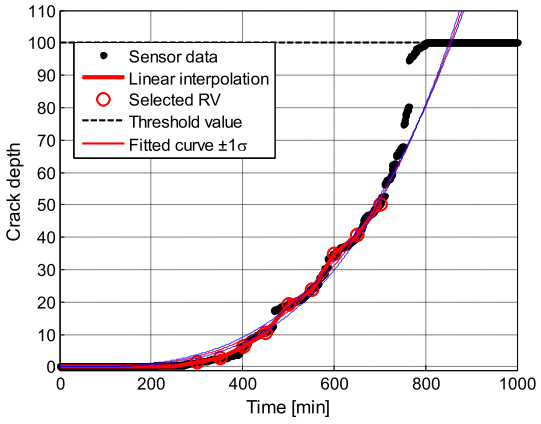

Fig. 18. Inspection time $T_{14} = 700$ (min).

and/or the associated noises are non-Gaussian (Djuric et al., 2003; Doucet et al., 2001). The method goes under the name of PF because the continuous distribution of the lifetime of the system of interest is approximated by a discrete set of weighed particles, where each particle represents a random trajectory of evolution in the state space and the weight is the probability of the trajectory.

FSBA is a data-driven fuzzy similarity based approach that uses data from failure dynamic scenarios of the system to create a library of reference trajectory patterns to failure. Given a failure scenario developing in the system, the remaining time before failure is predicted by comparing by fuzzy similarity analysis its evolution data to the reference trajectory patterns, and aggregating their times to failure in a weighted sum which accounts for their similarity to the developing pattern. The prediction of the failure time is dynamically updated as time goes by and measurements of signals representative of the system state are collected (Zio and Di Maio, 2010).

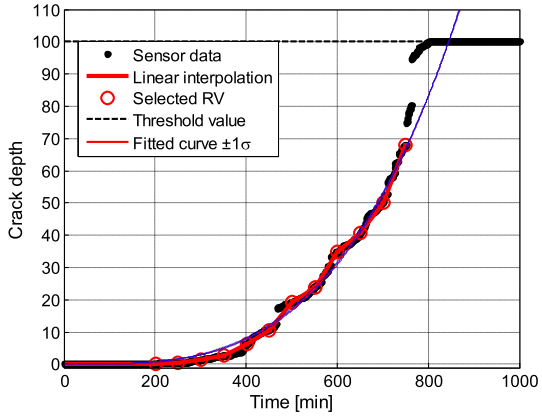

Fig. 19. Inspection time T_{15} = 750 (min).

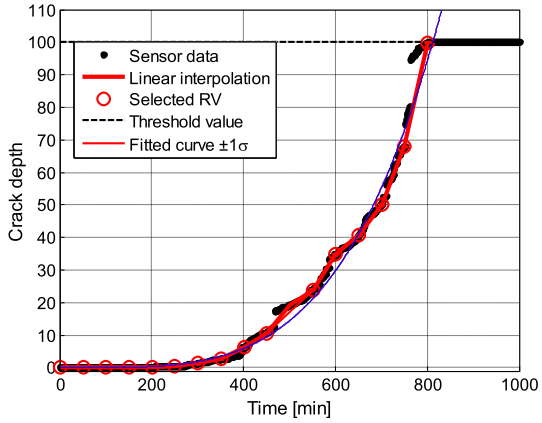

Fig. 20. Inspection time T_{16} = 800 (min).

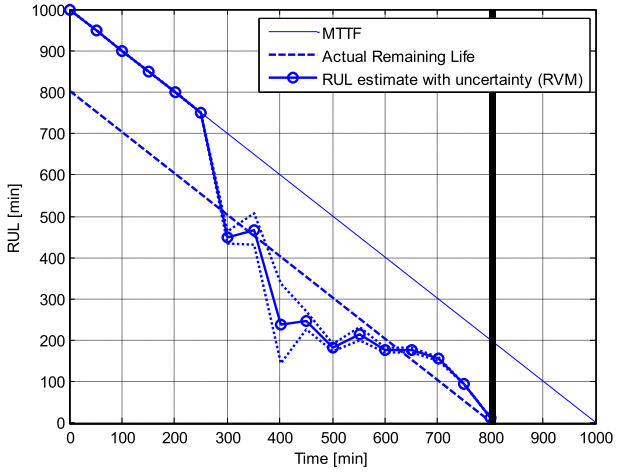

Fig. 21. RUL estimation for the crack propagation trajectory of Fig. 4.

Table 4 summarizes the quantitative results provided by the PF, FSBA and RVM approaches when the crack growth trajectory of Fig. 4 is used as test trajectory. The results show the good agreement of the RUL estimates (first, second and third column of Table 4) and the actual RUL (last column of Table 4) starting from time T_{det} = 300 (min), when the signal is detected to deviate from its nominal value.

It can be concluded that PF, FSBA and RVM are all suitable to tackle the problem of RUL estimation and they can be more or less

Table 3
Values of the estimated RUL $\hat{RUL}(T_j)$, its uncertainty interval $[\hat{RUL}_l(T_j)\ \hat{RUL}_u(T_j)]$ and the actual RUL $RUL(T_j)$ at time T_j.

Time T_j (min)	Estimated RUL $\hat{RUL}(T_j)$ (min)	Actual RUL $T^d - T_j$ (min)	Uncertainty interval 99% $[\hat{RUL}_l(T_j)\ \hat{RUL}_u(T_j)]$ (min)
0	1000	802	[1000 1000]
50	950	752	[950 950]
100	900	702	[900 900]
150	850	652	[850 850]
200	800	602	[800 800]
250	750	552	[750 750]
300 = T_{det}	448	502	[424 464]
350	466	452	[439 509]
400	237	402	[145 337]
450	246	352	[225 270]
500	180	302	[172 190]
550	215	252	[199 231]
600	176	202	[170 181]
650	175	152	[169 181]
700	154	102	[151 157]
750	95	52	[94 96]
800	12	2	[12 12]
802 = T	0	0	0

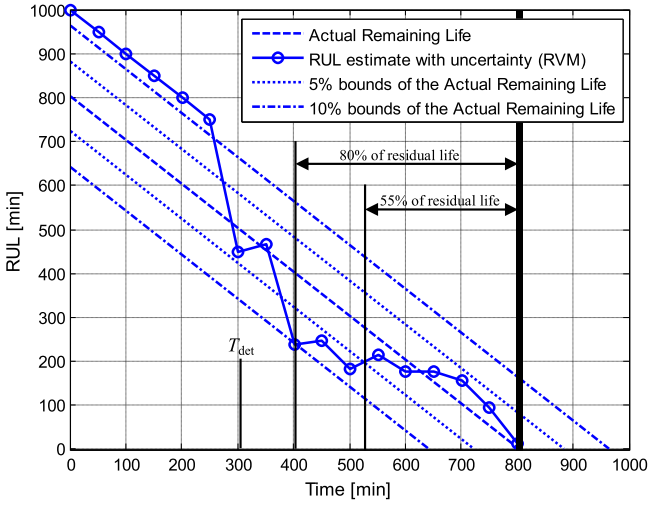

Fig. 22. Prognostic Horizon for the crack propagation trajectory of Fig. 4.

effective, depending on the quality and quantity of the available models and data. In this sense, the analyst is required to evaluate case-by-case the best approach in a trade-off between computational time and accuracy of predictions. In general terms of comparison (Table 5):

- PF allows uncertainty evaluation on the estimates of the RUL at the different inspection times when a detailed degradation model that takes into due account the physical properties of the degraded equipment is available and the model parameters can be estimated and updated from data (Cadini et al., 2009). With respect to FSBA and RVM, it requires longer computational times and a degradation model.
- FSBA is very fast and accurate in providing the estimation of the RUL when a large database of reference degradation trajectories is available for comparison with a newly developing degradation trajectory (Zio and Di Maio, 2010); it does not provide direct indication on the uncertainty of the RUL estimates.
- RVM allows the representation and propagation of the uncertainty in the RUL estimates and does not require a database of degradation patterns for similarity matching.

Table 4
Values of the RUL $\hat{RUL}(T_j)$ estimated with PF, FSBA and RVM approaches and the actual RUL $RUL(T_j)$ at time T_j.

Time T_j (min)	PF estimated RUL $\hat{RUL}(T_j)$ (min)	FSBA estimated RUL $\hat{RUL}(T_j)$ (min)	RVM estimated RUL $\hat{RUL}(T_j)$ (min)	Actual RUL $T^d - T_j$ (min)
0	1000	1000	1000	802
50	850	800	950	752
100	605	620	900	702
150	595	610	850	652
200	580	590	800	602
250	530	540	750	552
300 = T_{det}	490 Uncertainty interval 99% [395 608]	495	448 Uncertainty interval 99% [424 464]	502
350	432 Uncertainty interval 99% [377 578]	430	466 Uncertainty interval 99% [439 509]	452
400	376 Uncertainty interval 99% [145 433]	380	237 Uncertainty interval 99% [145 337]	402
450	340 Uncertainty interval 99% [225 418]	345	246 Uncertainty interval 99% [225 270]	352
500	292 Uncertainty interval 99% [172 390]	270	180 Uncertainty interval 99% [172 190]	302
550	220 Uncertainty interval 99% [115 331]	210	215 Uncertainty interval 99% [199 231]	252
600	185 Uncertainty interval 99% [105 281]	180	176 Uncertainty interval 99% [170 181]	202
650	182 Uncertainty interval 99% [105 258]	175	175 Uncertainty interval 99% [169 181]	152
700	145 Uncertainty interval 99% [98 177]	150	154 Uncertainty interval 99% [151 157]	102
750	90 Uncertainty interval 99% [45 196]	95	95 Uncertainty interval 99% [94 96]	52
800	10 Uncertainty interval 99% [8 20]	20	12 Uncertainty interval 99% [12 12]	2
802 = T	0	0	0	0

Table 5
Comparison of the performance of PF, FSBA and RVM methods.

	PF	FSBA	RVM
Computational CPU time	LARGE	SMALL	MEDIUM
Accuracy of predictions	HIGH	HIGH	HIGH
Uncertainty evaluation capability	YES	NO	YES
Necessity of database availability	NO	YES	NO
Accounting for physical properties	HIGH	LOW	MEDIUM
Necessity of a degradation model availability	YES	NO	YES

5. Conclusions

An original combination of RVM and model fitting has been proposed as a prognostic procedure for estimating the RUL of a component or structure, based on data collected on a single, undergoing degradation trajectory. The most relevant basis functions identified during the RVM learning procedure are fitted to the degradation model, which is then extrapolated to failure for estimating the RUL of the component or structure of interest.

The prognostic procedure has been applied to the crack propagation dynamics of a component or structure subject to fatigue cycles. The key features of the approach which have emerged for the application are the sparseness and the capability of uncertainty evaluation. The inferred predictors are indeed sparse in that they contain relatively few non-zero basis functions, i.e., relevant vectors (RVs); this allows making good predictions and avoiding over-fitting. On the other hand, RVM relies on a Bayesian framework, well suited to handle uncertainties through probability distributions over both parameters and variables; hence, the prediction results are provided with uncertainty intervals and the credibility of the results can be quantified by prognostic performance indicators, e.g., PH, a metric that ensures that the predicted estimates can be considered trustworthy.

The results obtained in the case study have been satisfactory from the point of view of both accuracy of the estimation and computing time. Furthermore, the procedure avoids the need of resorting to a fault detection module for the identification of the anomalous component or structure behavior: the algorithm proposed jointly detects the onset of the degradation-to-failure trajectory and performs the estimation of the available RT. The combination of RVM and model fitting has been shown to be a good candidate to be further investigated in the future for practical application.

Acknowledgments

We thank the anonymous referees for their thorough review, comments and suggestions that significantly contributed to improve the quality of the work.

This work was supported by the Science and Technology Fellowship Programme in China financed by the European Commission (Reference: EuropeAid/127024/L/ACT/CN).

References

Anderson, B. D., & Moore, J. B. (1979). *Optimal filtering*. Englewood Cliffs, NJ: Prentice Hall.

Barlett, E. B., & Uhrig, R. E. (1992). Nuclear power plant status diagnostics using an artificial neural network. *Nuclear Technology*, 97.

Baruah, P., & Chinnam, R. B. (2005). HMMs for diagnostics and prognostics in machining processes. *International Journal of Production Research, 43*(6), 1275–1293.

Bérenguer, C., Grall, A., & Castanier, B. (2000). Simulation and evaluation of condition based maintenance policies for multi-component continuous-state deteriorating systems. In M. Cottam, D. Harvey, R. Pape, J. Tait, (Eds.), *Proceedings of the foresight and precaution conference* (pp. 275–282).

Bigerelle, M., & Iost, A. (1999). Bootstrap analysis of FCGR, application to the Paris relationship and to lifetime prediction. *International Journal of Fatigue, 21*, 299–307.

Bolotin, V. V., Babkin, A. A., & Belousov, I. L. (1998). Probabilistic model of early fatigue crack growth. *Probabilistic Engineering Mechanics, 13*(3), 227–232.

Cadini, F., Zio, E., & Avram, D. (2009). Monte Carlo-based filtering for fatigue crack growth estimation. *Probabilistic Engineering Mechanics, 24*, 367–373.

Caesarendra, W., Niu, G., & Yang, B. S. (2010). Machine condition prognosis based on sequential Monte Carlo method. *Expert Systems with Applications, 37*(3), 2412–2420.

Caesarendra, W., Widodo, A., & Yang, B. S. (2010). Application of relevance vector machine and logistic regression for machine degradation assessment. *Mechanical Systems and Signal Processing, 24*, 1161–1171.

Campolucci, P., Uncini, A., Piazza, F., & Rao, B. D. (1999). On-line learning algorithms of locally recurrent neural networks. *IEEE Transactions on Neural Networks, 10*, 253–271.

Castanier, B., Bérenguer, C., & Grall, A. (2002). Stochastic maintenance planning for a repairable system which is inoperative during maintenance operations. In E. J. Bonano, A. L. Camp, M. J. Majors, & R. A. Thompson (Eds.). *Probabilistic safety assessment and management, PSAM6* (pp. 1365–1370). Amsterdam: Elsevier.

Chen, D., & Trivedi, K. S. (2005). Optimization for condition-based maintenance with semi-Markov decision process. *Reliability Engineering & System Safety, 90*, 25–29.

Chiang, L. H., Russel, E., & Braatz, R. (2001). *Fault detection and diagnosis in industrial systems*. London: Springer-Verlag.

Djuric, P. M., Kotecha, J. H., Zhang, J., Huang, Y., Ghirmai, T., Bugallo, M. F., et al. (2003). Particle filtering. *IEEE Signal Process*, 19–37.

Dong, M., & He, D. (2007). Hidden semi-Markov model-based methodology for multi-sensor equipment health diagnosis and prognosis. *European Journal of Operational Research, 178*(3), 858–878.

Doucet, A. (1998). *On sequential simulation-based methods for Bayesian filtering*. Technical report, CUED-F-ENGTR310. Department of Engineering, University of Cambridge.

Doucet, A., de Freitas, J. F. G., & Gordon, N. J. (2001). An introduction to sequential Monte Carlo methods. In A. Doucet, J. F. G. de Freitas, & N. J. Gordon (Eds.), *Sequential Monte Carlo in practice*. New York: Springer-Verlag.

Doucet, A., Godsill, S., & Andreu, C. (2000). On sequential Monte Carlo sampling methods for Bayesian filtering. *Statistics and Computing, 10*, 197–208.

Drucker, H., Burges, C. J. C., Kaufman, L., Smola, A., & Vapnik, V. (1997). Support vector regression machines. *Advances in Neural Information Processing Systems, 9*, 155–161.

Fletcher, T. (2008). *Relevance vector machines explained*. <www.cs.ucl.ac.uk/staff/T.Fletcher>.

Goebel, K., & Bonissone, P. (2005). Prognostic information fusion for constant load systems. In *Proceedings of the 7th annual conference on information fusion* (Vol. 2, pp. 1247–1255).

Grall, A., Bérenguer, C., & Chu, C. (1998). Optimal dynamic inspection/replacement planning in condition-based maintenance. In S. Lydersen, G. Hansen, H. Sandtorv, (Eds.), *Proceedings of the European safety and reliability conference, ESREL'98* (pp. 381–388).

Hontelez, J. A. M., Burger, H. H., & Wijnmalen, D. J. D. (1996). Optimum condition-based maintenance policies for deteriorating systems with partial information. *Reliability Engineering & System Safety, 51*, 267–274.

Hyndman, R. J., & Koehler, A. B. (2006). Another look at measures of forecast accuracy. *International Journal of Forecasting, 22*, 679–688.

Jardine, A. K. S., Lin, D., & Banjevic, D. (2006). A review on machinery diagnostics and prognostics implementing condition based maintenance. *Mechanical Systems and Signal Processing, 20*, 1483–1510.

Kitagawa, G. (1987). Non-Gaussian state-space modeling of nonstationary time series. *Journal of the American Statistical Association, 82*, 1032–1063.

Kopnov, V. A. (1999). Optimal degradation process control by two-level policies. *Reliability Engineering & System Safety, 66*, 1–11.

Kozin, F., & Bogdanoff, J. L. (1989). Probabilistic models of fatigue crack growth: Results and speculations. *Nuclear Engineering and Design, 115*, 143–171.

Lam, C., & Yeh, R. (1994). Optimal maintenance policies for deteriorating systems under various maintenance strategies. *IEEE Transactions on Reliability, 43*, 423–430.

Makridakis, S., & Hibon, M. (2000). The M3-competition: Results, conclusions and implications. *International Journal of Forecasting, 16*, 451–476.

Marseguerra, M., Zio, E., & Podofillini, L. (2002). Condition-based maintenance optimization by means of genetic algorithms and Monte Carlo simulation. *Reliability Engineering & System Safety, 77*, 151–165.

More, A., & Deo, M. C. (2003). Forecasting wind with neural networks. *Marine Structures, 16*, 35–49.

Myotyri, E., Pulkkinen, U., & Simola, K. (2006). Application of stochastic filtering for lifetime prediction. *Reliability Engineering & System Safety, 91*, 200–208.

Oswald, G. F., & Schueller, G. I. (1984). Realiability of deteriorating structures. *Engineering Fracture Mechanics, 20*(1), 479–488.

Peel, L. (2008). Data driven prognostics using a Kalman filter ensemble of neural network models. In *International conference on prognostics and health management*.

Provan, J. W. (Ed.). (1987). *Probabilistic fracture mechanics and reliability*. Martinus: Nijhoff Publishers.

Pulkkinen, U. (1991). A stochastic model for wear prediction through condition monitoring. In K. Holmberg & A. Folkeson (Eds.), *Operational reliability and systematic maintenance* (pp. 223–243). London, New York: Elsevier.

Pulkkinen, U., & Uryas'ev, S. (1992). Optimal operational strategies for an inspected component. In K. E. Petersen & B. Rasmussen (Eds.), *Safety and reliability'92, proceedings of the European safety and reliability conference'92* (pp. 896–907). London: Elsevier.

Samanta, P. K., Vesely, W. E., Hsu, F., & Subudly, M. (1991). *Degradation modeling with application to ageing and maintenance effectiveness evaluations*, NUREG/CR-5612. US Nuclear Regulatory Commission.

Santosh, T. V., Srivastava, A., Sanyasi Rao, V. V. S., Gosh, A. K., & Kushwaha, H. S. (2009). Diagnostic system for identification of accident scenarios in nuclear power plants using artificial neural networks. *Reliability Engineering & System Safety, 94*, 759–762.

Saxena, A., Celaya, J., Saha, B., Saha, S., & Goebel, K. (2009). Evaluating algorithm performance metrics tailored for prognostics. In *IEEE aerospace conference, Big Sky MT* (pp. 1–13).

Simola, K., & Pulkkinen, U. (1998). Models for non-destructive inspection data. *Reliability Engineering & System Safety, 60*, 1–12.

Sobezyk, K., & Spencer, B. F. (1992). *Random fatigue: From data to theory*. Boston, MA: Academic Press.

Sotiris, V., & Pecht, M. (2007). Support vector prognostics analysis of electronic products and systems. In *The AAAI conference on artificial intelligence*.

Tipping, M. E. (2001). Sparse Bayesian learning and the relevance vector machine. *Journal of Machine Learning Research, 1*, 211–244.

Tran, V. T., Yang, B. S., & Tan, A. C. C. (2009). Multi-step ahead direct prediction for the machine condition prognosis using regression trees and Neuro-Fuzzy systems. *Expert Systems with Applications, 36*(5), 9378–9387.

Vachtsevanos, G., Lewis, F. L., Roemer, M., Hess, A., & Wu, B. (2006). *Intelligent fault diagnosis and prognosis for engineering systems* (1st ed.). Hoboken, New Jersey: John Wiley and Sons, Inc.

Vlok, P. J., Coetzee, J. L., Banjevic, D., Jardine, A. K. S., & Makis, V. (2002). An application of vibration monitoring in proportional hazards models for optimal component replacement decisions. *Journal of the Operational Research Society, 53*, 193–202.

Wang, T., Yu, J., Siegel, D., & Lee, J. (2008). A similarity based prognostic approach for remaining useful life estimation of engineered systems. In *International conference on prognostics and health management*.

Wang, W. Q., Goldnaraghi, M. F., & Ismail, F. (2004). Prognosis of machine health condition using Neuro-Fuzzy systems. *Mechanical Systems and Signal Processing, 18*, 813–831.

Williams, J. H., Davies, A., & Drake, I. R. (1994). *Condition-based maintenance and machine diagnostics*. Chapman and Hall, p. 187, ISBN: 0 4 I2465 00 0.

Yan, J., Koç, M., & Lee, J. (2004). A prognostic algorithm for machine performance assessment and its application. *Production Planning & Control, 15*(8), 796–801.

Yeh, R. H. (1997). State-age-dependent maintenance policies for deteriorating systems with Erlang sojourn time distributions. *Reliability Engineering & System Safety, 58*, 55–60.

Zio, E., & Di Maio, F. (2010). A data-driven fuzzy approach for predicting the remaining useful life in dynamic failure scenarios of a nuclear system. *Reliability Engineering & System Safety, 95*(1), 49–57. http://dx.doi.org/10.1016/j.ress.2009.08.001.